esa

ECOSPHERE

Using canopy greenness index to identify leaf ecophysiological traits during the foliar senescence in an oak forest

Zhunqiao Liu,[1,2] Shuqing An,[1] Xiaoliang Lu,[2,3] Haibo Hu,[4] and Jianwu Tang[2,]†

[1]*School of Life Sciences, Nanjing University, Nanjing, Jiangsu 210037 China*
[2]*The Ecosystems Center, Marine Biological Laboratory, Woods Hole, Massachusetts 02543 USA*
[3]*Department of Forest Ecosystems and Society, Oregon State University, Corvallis, Oregon 97331 USA*
[4]*Collaborative Innovation Center of the Southern Modern Forestry, Nanjing Forestry University, Nanjing 210037 China*

Citation: Liu, Z., S. An, X. Lu, H. Hu, and J. Tang. 2018. Using canopy greenness index to identify leaf ecophysiological traits during the foliar senescence in an oak forest. Ecosphere 9(7):e02337. 10.1002/ecs2.2337

Abstract. Camera-based observation of forest canopies allows for low-cost, continuous, high temporal-spatial resolutions of plant phenology and seasonality of functional traits. In this study, we extracted canopy color index (green chromatic coordinate, G_{cc}) from the time-series canopy images provided by a digital camera in a deciduous forest in Massachusetts, USA. We also measured leaf-level photosynthetic activities and leaf area index (LAI) development in the field during the growing season, and corresponding leaf chlorophyll concentrations in the laboratory. We used the Bayesian change point (BCP) approach to analyze G_{cc}. Our results showed that (1) the date of starting decline of LAI (DOY 263), defined as the start of senescence, could be mathematically identified from the autumn G_{cc} pattern by analyzing change points of the G_{cc} curve, and G_{cc} is highly correlated with LAI after the first change point when LAI was decreasing (R^2 = 0.88, LAI < 2.5 m^2/m^2); (2) the second change point of G_{cc} (DOY 289) started a more rapid decline of G_{cc} when chlorophyll concentration and photosynthesis rates were relatively low (13.4 ± 10.0% and 23.7 ± 13.4% of their maximum values, respectively) and continuously reducing; and (3) the third change point of G_{cc} (DOY 295) marked the end of growing season, defined by the termination of photosynthetic activities, two weeks earlier than the end of G_{cc} curve decline. Our results suggested that with the change point analysis, camera-based phenology observation can effectively quantify the dynamic pattern of the start of senescence (with declining LAI) and the end of senescence (when photosynthetic activities terminated) in the deciduous forest.

Key words: chlorophyll; digital camera; leaf area index; phenology; photosynthesis; senescence.

Received 18 December 2017; revised 22 May 2018; accepted 25 May 2018. Corresponding Editor: Dawn M. Browning.

† **E-mail:** jtang@mbl.edu

Introduction

Phenological change of temperate deciduous forest ecosystems exerts a strong feedback to the global carbon balance through annual fluctuations of photosynthesis in its duration and strength, evapotranspiration, and land surface albedo (Lieth 1974, Piao et al. 2008, Penuelas et al. 2009, Richardson 2012). Climate change is currently altering the timing of plant phenological phases, such as the start and end date of bud-break, leaf expansion, and senescence, as temperature and precipitation changes (Menzel 2002, Vitasse et al. 2009, Chen and Xu 2012, Yang et al. 2012, Fu et al. 2015). Long-term phenological observation of forest canopies is likely to improve understanding of the relationship between terrestrial ecosystem dynamics and climate change, and to monitor the impact of climate change on ecosystem function (Brown et al. 2016, Liu et al. 2016, Tang et al. 2016).

To meet the requirements of low-cost, stable, and accurate phenological observation of canopies, digital repeat photography, which was continuously captured by tower mounted time-lapse digital cameras, provides phenological information with high temporal and spatial resolutions. It provides phenological information with high temporal and spatial resolutions (Richardson et al. 2007, Ide and Oguma 2010, Sonnentag et al. 2012, Brown et al. 2016). Seasonal changes in canopy color indices (such as green chromatic coordinate, G_{cc}), extracted from the region of interest (ROI) in repeat canopy photography, were closely related to seasonal changes in phenology of deciduous forests, such as bud-break, leaf expansion, and leaf abscission (Woebbecke et al. 1995, Richardson et al. 2009, Sakamoto et al. 2012, Ide and Oguma 2013, Keenan et al. 2014, Filippa et al. 2015, Moore et al. 2016, Nagai et al. 2016). In addition, G_{cc} can track plant physiological characters, such as leaf area index (LAI; Ryu et al. 2012, Liu et al. 2015), leaf chlorophyll concentration (Keenan et al. 2014, Yang 2014), and gross primary production (GPP; Ahrends et al. 2009, Mizunuma et al. 2014, Wingate et al. 2015, Yang et al. 2016), even though mismatches between G_{cc} and chlorophyll concentration may exist (Yang et al. 2017). Based on the widespread application of canopy repeat imagery, regional camera-based phenological networks were initiated and extended, such as the PhenoCam Network (Richardson et al. 2009, 2018), the National Ecological Observatory Network (Kampe et al. 2010), EUROPheno Network (Wingate et al. 2015), Phenological Eyes Network (PEN; Nasahara and Nagai 2015), and Australian Phenocam Network (Moore et al. 2016). These networks cooperate with other ecological research networks and provide integrated monitoring data to further study dynamics and function of terrestrial ecosystems.

Camera-based phenological observation methods open a promising prospect for studying seasonal and annual dynamics in both canopies and leaves, though there remains a need to integrate imagery information to further understand timing of phenological shifts and plant physiological traits, especially during autumn (Inoue et al. 2014, Keenan et al. 2014, Nagai et al. 2015). Canopy phenology in early spring, including bud-break, leaf-out, and blossom, can be detected by manual or camera observations. For example, rapid increases in G_{cc} typically represent the start of canopy leaf-out in spring (Richardson et al. 2009, Keenan et al. 2014). Depending on how the start of the growing season is defined (by increasing LAI or chlorophyll concentration), the spring curve of G_{cc} could well represent the development of LAI (Liu et al. 2015), but the peak of G_{cc} could be a ~3 weeks earlier than the peak of the chlorophyll concentration in the deciduous forest (Yang et al. 2014). Compared with the spring leaf-out, plant senescence, initiated by biochemical processes, is more difficult to track by digital cameras because senescence could start earlier than changes in leaf color and abscission that may occur during the final stage of senescence (Tang et al. 2016). Multiple factors may contribute uncertainty in detecting and predicting senescence in canopies. For example, Nagai et al. (2015) showed that heterogeneous distribution, year-to-year variability, and different leaf change patterns caused large uncertainty in detecting the date of leaf fall. Keenan et al. (2014) demonstrated that color indices were insensitive to changes in physiological traits under high LAI and chlorophyll concentration levels. Inoue et al. (2014) argued that the end of leaf-off is more variable than the beginning of leaf expansion in the spring. Yang et al. (2014) found that the canopy redness index was strongly correlated with the change of pigments concentrations during the senescence. Further examination of G_{cc} and other physiological traits during the senescence period will improve understanding of how canopy growing seasons vary with environmental conditions.

Photosynthetic activity is one of the most important ecophysiological functions that are influenced by phenology. Positive correlations between seasonal photosynthesis activity and G_{cc} have been reported based on canopy eddy covariance measurements and repeat digital photography observations in both deciduous forest and grassland (Toomey et al. 2015, Browning et al. 2017, Matiu et al. 2017, Westergaard-Nielsen et al. 2017). Using simply measured G_{cc} to track seasonality of photosynthesis will provide a great advantage over manual inspection in recording photosynthesis dynamics and supporting modeling of carbon cycling over the season. Long-term and continental networks for camera-based

phenology observation, when coupled with field-based leaf ecophysiological measurements, will allow for the functional validation canopy greenness indices in diverse land ecosystems.

The seasonal pattern of G_{cc} has been manually described to match the dynamics of LAI or photosynthesis (Yang et al. 2014). To overcome the uncertainty of manual observations from time-series curves and the unrealistic asymptotic assumptions in logistic model fits (Henneken et al. 2013), the Bayesian change point (BCP) analysis has been used to mathematically detect G_{cc}. Bayesian change point analysis could detect small curve changes that indicate the initial change of physiological traits, but these changes may not be reflected by the logistic fitting. In this study, we assess how repeat canopy photography varies with a variety of canopy physiological and structural factors, including leaf-level photosynthetic rate, LAI, leaf pigments concentrations, canopy green rate, and defoliation rate, during autumn senescence in a temperate white oak (*Quercus alba*) dominated forest. We detected the start and end time of senescence using the BCP analysis for G_{cc}.

Methods

Research site

All measurements and observations were conducted during the autumn of 2013 (from September to November) in a deciduous forest dominated by white oak (*Quercus alba*), located at the Manuel F. Correllus State Forest (41°21′42.74″ N, 70°34′41.67″ W) on the island of Martha's Vineyard, Massachusetts, USA (Yang et al. 2014). The white oak forest is approximately 100 yr old, reforested from abandoned agricultural land (Foster et al. 2002). This site is characterized by a humid continental climate. The annual average temperature increased from March to July and then decreased till February 2014, ranging between −1.5° and 24.2°C during that period. Annual precipitation was 1,181 mm in 2013. Monthly total precipitation varied from 8 to 168 mm, with <20 mm in September and October, but more than 60 mm in other months.

Canopy images

To observe phenological change of the white oak forest, we installed a digital camera (NetCam SC 1.3MP, StarDot, Buena Park, California, USA) on a 15-m tower. The camera had been set up toward the north and downward 15° from the horizontal surface to obtain a wide visual view of the plant canopy. Each day, canopy images were taken hourly between 10:00 and 15:00 hours during the period from August and November, recorded as a JPEG format with a resolution of 1296 × 960 pixels and saved on a local server (TS-U100, USB Network Storage Server, TRENDnet, Torrance, California, USA). The camera and local server were powered by the field solar panel system (Yang et al. 2014).

Repeat canopy images were processed by the following procedures: First, we manually inspected and excluded contaminated canopy images that were captured during extreme weather conditions, such as heavy fog, rain, and overexposed sky. Second, we selected the region of interest (ROI) to analyze the greenness index of images from the same field of view area where we measured the leaf area index (LAI) and leaf pigments (Fig. 1, in details below). Third, we used the PhenoCam GUI which is an application developed by Phenocam (https://phenocam.sr.unh.edu/webcam/) to extract the average digital number for red, green, and blue color channels, and then calculated the green chromatic coordinate (G_{cc}; Eq. 1). In contrast to original RGB digital number, the color index of G_{cc} could reduce the effect of scene illumination and more clearly demonstrate color change on plant canopy (Woebbecke et al. 1995, Richardson et al. 2009, Sonnentag et al. 2012).

$$G_{cc} = \frac{\text{greenDN}}{\text{redDN} + \text{greenDN} + \text{blueDN}} \quad (1)$$

Here, G_{cc} is the index of green chromatic coordinates; redDN, greenDN, and blueDN represent the average digital number of red, green, and blue channel in user-defined ROI.

Fourth, the timing of the phenological transition was determined by tracking change points in G_{cc} time-series. In this study, the BCP-based approach was used to identify change points (Yang 2014). Specifically, a hierarchical model was constructed as follows: A logit transform was first applied to G_{cc} time-series, and the transformed data were assumed to follow a logit-normal distribution. Next, the expectation of the

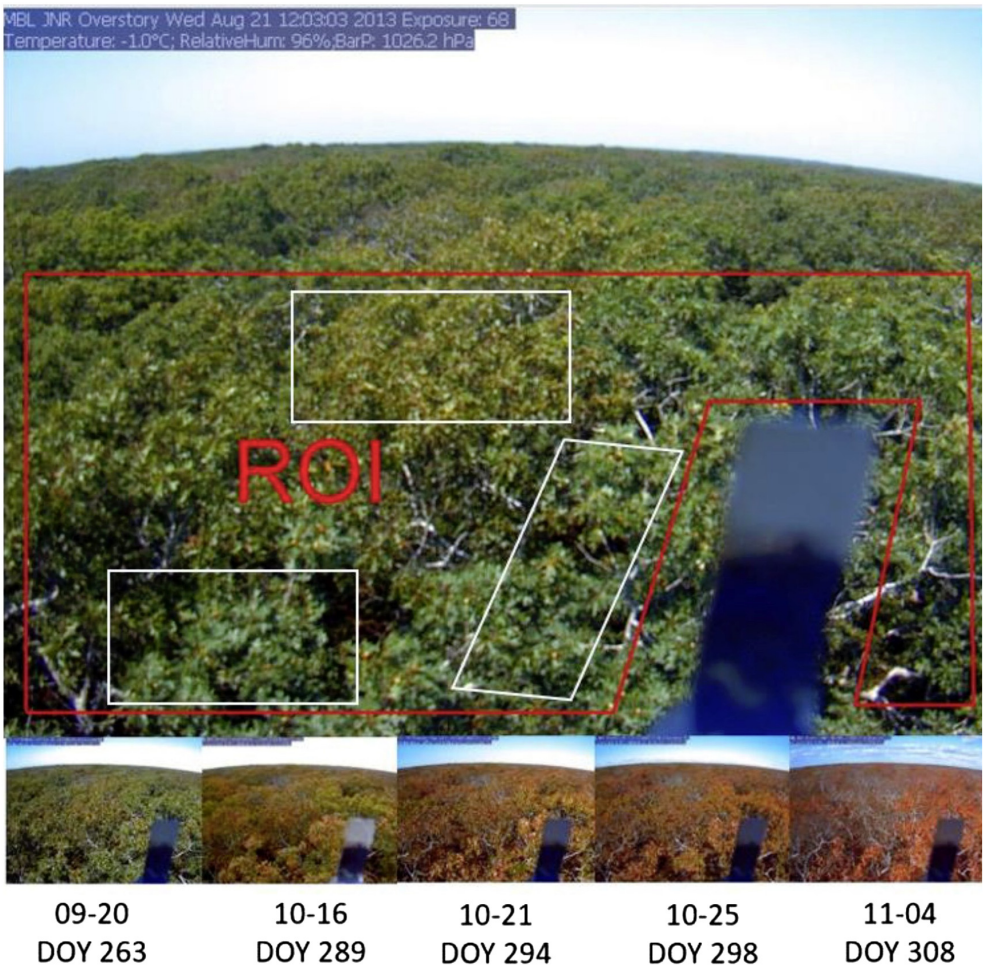

Fig. 1. An example of the time-serial images from the white oak canopy. The red polygon was the region of interest (ROI) used to calculate G_{cc}. The white rectangle lines identified the top canopies of the three trees. Bottom images are the typical plant situations in different times of foliar senescence (time format: mm-dd, the day of year, DOY).

logit-normal distribution was modeled as the normal distribution based on the piecewise linear regression which fit the logit transform G_{cc} time-series and provided intercepts and slopes for these fitted lines. Furthermore, the prior distributions of model parameters which controlled the piecewise linear regression were set based on the seasonal maximum and minimum value of the transformed logit G_{cc}. Then, the posterior probabilities of all possible piecewise linear regression models were assessed by reversible jump Markov Chain Monte Carlo sampling (MCMC). This hierarchical model was able to calculate the posterior probability of the number of change points and the posterior probability of a certain day which is a change point, and thus identify the locations of the change points and its uncertainty. In summary, the BCP-based approach can quantify the change points on the slope of G_{cc} time-series, which fits the time-series with piecewise linear regressions and identifies the endpoints of each linear segmentation (Thomson et al. 2010, Henneken et al. 2013, Pope et al. 2013, Yang et al. 2014, Liu et al. 2015). Therefore, compared with fitting logistic curves, the BCP method could detect the curve change point without smoothing fit curve that may lead to biases in the analyses of phenology transition

phases. In this study, we used BCP analysis to identify key phenological transition dates during the senescence along the time-series data obtained from the camera imagery.

Measurements of canopy biochemical and structure properties

In order to examine the relationship between the change of G_{cc} and canopy structure and biochemical properties transformation, a high temporal resolution dataset of LAI, leaf photosynthetic rate, and foliar pigments concentrations were measured during the period of defoliation (09/16–11/04). Leaf samples were collected on 5-d intervals from the three white oak trees, which located in the ROI, throughout the defoliation period.

We labeled two leaf branches in each tree and randomly chose three intact green leaves, located in the lower canopy level around the high platform, to measure the maximum photosynthetic rate (μmol $CO_2 \cdot m^{-2} \cdot s^{-1}$) with the LI-6400 portable photosynthesis system (LI-COR, Lincoln, Nebraska, USA). We chose the 6400-02B LED as the light source and measured the light response curves with a decreasing sequence of photosynthetically active radiation, or PAR, (2000, 1500, 1000, 500, 200, 50, 20 and 0 μmol·$m^{-2} \cdot s^{-1}$) as the in-chamber light intensity. Based on the field measurements (Fig. 2), the photosynthetic rate remained saturated when PAR is larger than 1000 μmol·$m^{-2} \cdot s^{-1}$. Therefore, we considered the photosynthetic rate when PAR >1000 μmol·$m^{-2} \cdot s^{-1}$as the maximum net photosynthetic rate (A_{net}, μmol $CO_2 \cdot m^{-2} \cdot s^{-1}$) for each sampling leaf, and also assumed that photosynthetic rate in the dark chamber when PAR = 0 μmol $CO_2 \cdot m^{-2} \cdot s^{-1}$ as the mitochondrial dark respiratory rate (R_{dark}). Then, the maximum photosynthetic rate (A_{max}, μmol $CO_2 \cdot m^{-2} \cdot s^{-1}$) was calculated by the following equation (Eq. 2). We calculated the whole canopy maximum photosynthetic rate (C_A_{max}, μmol $CO_2 \cdot m^{-2} \cdot s^{-1}$) by multiplying the rate of green leaves in the canopy (LAI_G) and A_{max} (see Eqs. 9 and 11). Note that A_{max} was measured on the green leaves unless there were not green leaves at the end of senescence. The time of the end of

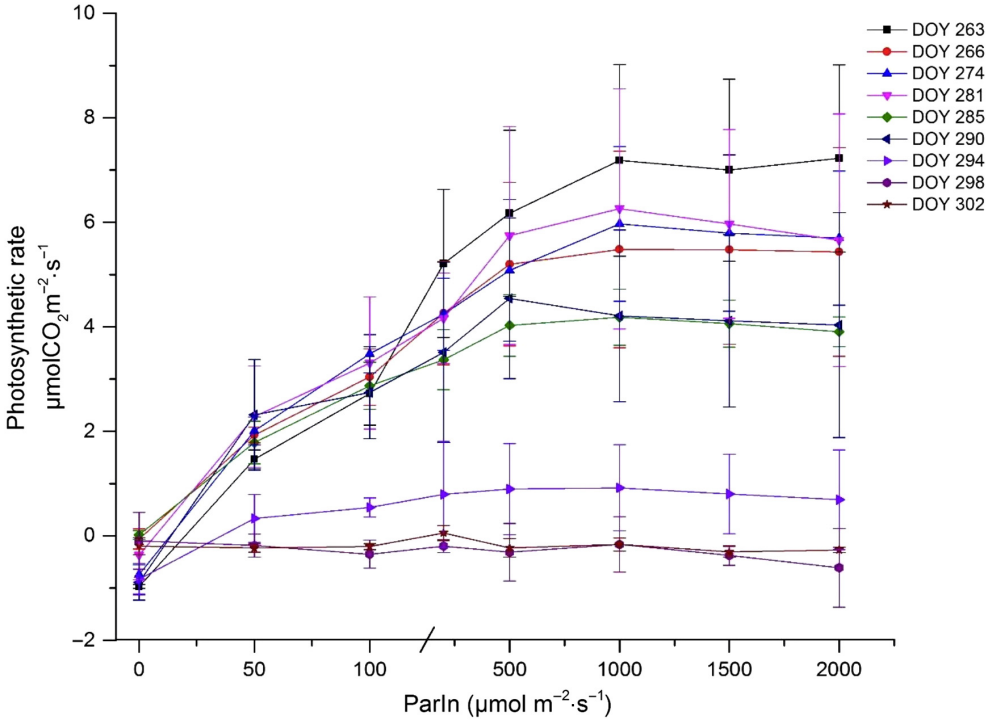

Fig. 2. The light response of photosynthetic rate in different dates of foliar senescence, which were measured by Li-cor 6400 XT in the light intensity of 2000, 1500, 1000, 500, 200, 50, 20, and 0 μmol·$m^{-2} \cdot s^{-1}$.

growing season was defined as the date when measured C_A_{max} was lower than the 10% of maximum C_A_{max} during the autumn experiment campaign.

$$A_{max} = A_{net} + R_{dark} \quad (2)$$

$$C\_A_{max} = LAI_G \times A_{max} \quad (3)$$

We used a tree pruner to randomly cut one leaf branch from the high, middle, and low levels of the canopy for each tree; then, three leaves were randomly selected in each branch and immediately placed in a zip bag that contained a moist paper towel to keep water loss from the leaf. All leaf samples were reserved in the ice-filled cooler to reduce water and pigment loss (Foley et al. 2006). After two hours, we returned to the laboratory and used a hole punch (diameter 0.635 cm) to get multiple leaf disks (0.32 cm^2 each). We randomly chose three intact leaf disks for grinding in a mortar with 100% acetone solution and magnesium oxide (MgO) mixture (Asner et al. 2009), added acetone/MgO mixture till 5 milliliters, centrifuged 8 minutes, and measured the absorbance of the supernatant with a spectrophotometer (Shimadzu UV-1201, Kyoto, Japan). We calculated the chlorophyll a, b, and carotenoids concentrations (Chl *a*, Chl *b*, and Car) through the readings from 470, 662, and 645 nm (A_{470}, A_{662}, and A_{645}) using the following equations (Eqs. 4, 5, and 6; Lichtenthaler and Buschmann 2001, Yang et al. 2014).

$$\text{Chl } a\ (\mu g/cm^2) = (11.24 \times A_{662} - 2.04 \times A_{645}) \times \frac{5}{3 \times 0.32} \quad (4)$$

$$\text{Chl } b\ (\mu g/cm^2) = (20.13 \times A_{645} - 4.19 \times A_{662}) \times \frac{5}{3 \times 0.32} \quad (5)$$

$$\text{Car}\ (\mu g/cm^2) = (1000 \times A_{470} - 1.90 \times \text{Chl } a - 63.14 \times \text{Chl } b) \times \frac{5}{3 \times 0.32} \quad (6)$$

$$\text{Chl}\ (\mu g/cm^2) = \text{Chl } a + \text{Chl } b \quad (7)$$

To count the percentage of leaf color change, we randomly labeled three branches located in the canopy, counted the total number of leaves ($Leaf_T$, %) and the number of discolored leaves ($Leaf_D$, %) in these branches, and used the first time counted foliar number as the maximum number of leaves ($Leaf_M$, %). We then calculated leaf-on rate ($Leaf_O$, %) and leaf-green rate ($Leaf_G$, %) on the branches by using the following equations:

$$Leaf_O = 100 \times \frac{Leaf_T}{Leaf_M} \quad (8)$$

$$Leaf_G = 100 \times \frac{Leaf_T - Leaf_D}{Leaf_T} \quad (9)$$

Ten open boxes (0.20 m^2) were randomly placed under the canopy in August, located within the ROI, to collect fallen leaves at the same sampling frequency to Chl. All the fallen leaves in each box were collected and measured the leaves dry mass (DM_i) after staying in the 70°C drying oven for 72 h. We then calculated the canopy leaf-fall rate ($Leaf_F$) with the following equation (Eq. 10):

$$Leaf_F = 100 \times \frac{\sum_{i=1}^{k} DM_i}{\sum_{i=1}^{n} DM_i} \quad (10)$$

where k and n were ordinal sampling numbers and total sampling numbers, respectively.

LAI was measured by the LAI-2000 Plant Canopy Analyzer (LI-COR, Lincoln, Nebraska, USA) within ROI at the same time of leaf sampling. We assumed the measurement of LAI in January 2014 when the forest was dormant as the background value (LAI_B) and then used the measured LAI value minus LAI_B for calculating actual LAI of the forest canopy. The start date of senescence is defined in this study as the start of LAI decrease. Further, we assumed the rate of green leaves in the canopy could be represented by multiplying the value of the actual LAI and $Leaf_G$ (Eq. 11).

$$LAI_G = LAI \times Leaf_G \quad (11)$$

Results

The camera-based index of the forest canopy, G_{cc}, showed a declining trend in the deciduous forest in the autumn (Keenan et al. 2014, Brown et al. 2016; Fig. 3e). Based on the result of BCP analysis for the downward-trending G_{cc} curve (Fig. 3e), we found three major change points

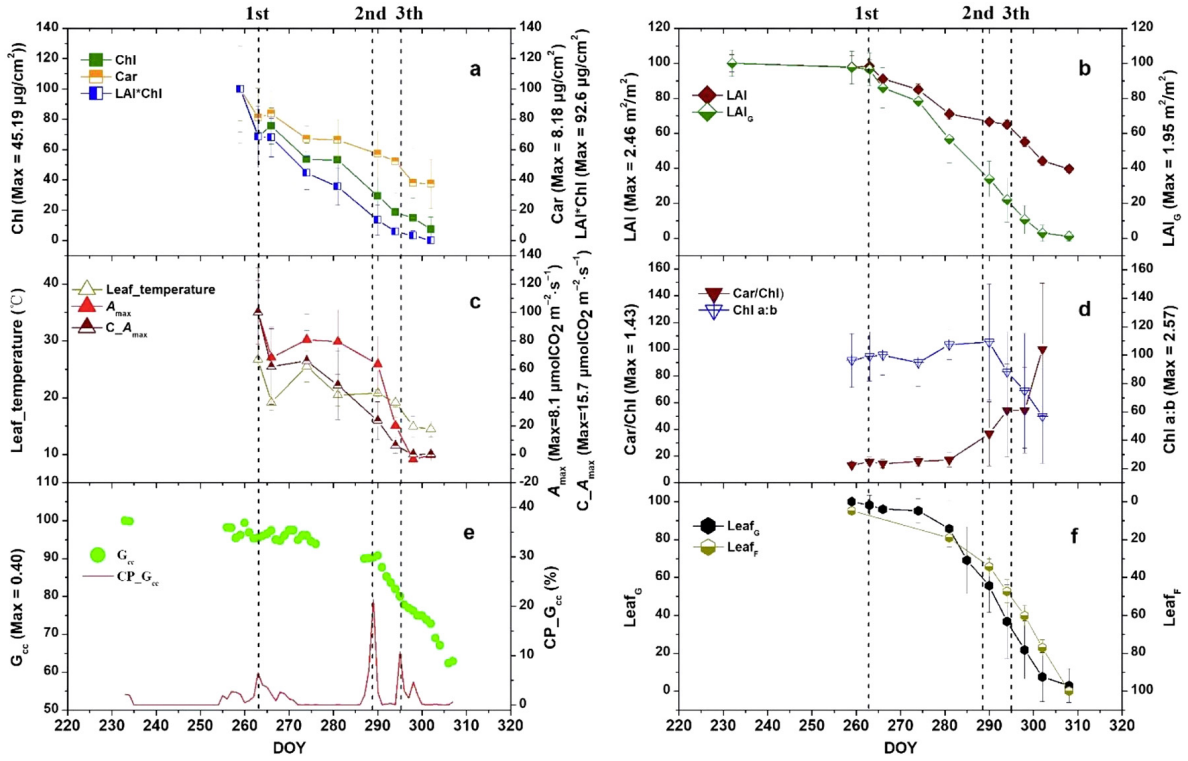

Fig. 3. Comparisons between the color index, pigments concentration, leaf area index, photosynthesis rate, and $Leaf_F$ rate. The dashed black lines indicate three days of change points during the senescence period. (a) The percentage curve of total chlorophyll and carotenoids concentration to their maximum; (b) the percentage curve of LAI and LAI_G (LAI multiplying the $Leaf_G$ rate in Fig. 3f) to each maximum value; (c) the percentage curve of A_{max}, which is the maximum rates of photosynthesis per unit foliage area at saturating irradiance, on the labeled branches. The percentage curve of LAI_G multiplies the foliar Amax to itself maximum and the curve of leaf temperature when measured the A_{max}; (d) similar with the Fig. 3a, but with the indices of the ratio of carotenoids to total chlorophyll concentration and the ratio of chlorophyll a to chlorophyll b; (e) the percentage curve of G_{cc} and probability of change point of $G_{cc;}$ (f) the ratio of counting a number of green leaves to initial foliar number on the 12 labeled branches, and the ratio of foliar weight collected by 10 boxes to each total weight after finishing all collection.

of the time-series G_{cc}, occurring on DOY 263, 289, and 295, respectively. We identified these change points according to the order of time sequence. Fig. 3e also demonstrated that the G_{cc} curve remained generally flat before DOY 263. Then, G_{cc} showed a slight decline between DOY 263 and DOY 289 and a much more rapid decrease after DOY 289. A more moderate rate of the decrease occurred after DOY 294. On the other hand, fitting logistic curve shows that the start of senescence, the middle of senescence, and the end of senescence occurred on DOY 288, 295, and 302, respectively (Fig. 4). Compared with the BCP analysis, the start of senescence and the end of senescence with fitting the logistic curve delayed 15 and 7 d, respectively.

The light response curve of photosynthesis showed that the rate of leaf photosynthesis kept the constant level close to the A_{max} (the maximum rate of photosynthesis at saturating irradiance) when photosynthetically active radiation (PAR) was larger than 1000 $\mu mol \cdot m^{-2} \cdot s^{-1}$ (Fig. 2). Though Chl concentration declined, the rates of A_{max} varied with leaf temperature from DOY 264 to DOY 281 (Fig. 3a, c). After that, A_{max}

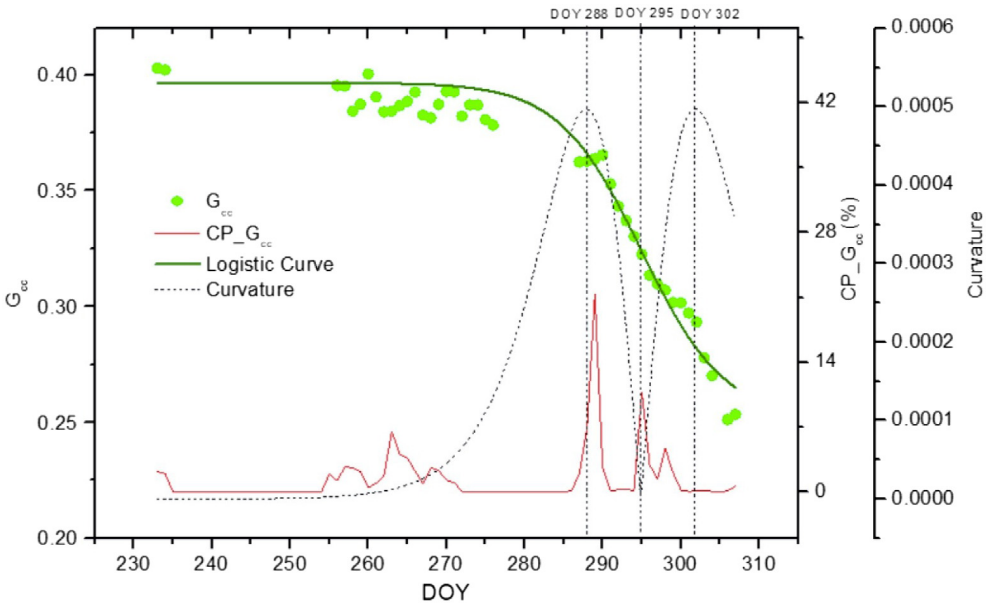

Fig. 4. Illustration of estimating the autumn phenological phases based on the logistical fitting and its curvature. Green dots are the daily G_{cc} value, the red solid line is the probability of change point of G_{cc} based on the Bayesian change point (BCP) approach, the dark green solid line is the G_{cc} fitted logistics curve, and the black dash line is the curvature of the fitting curve. Black dash vertical lines are the three phenological phases at DOY 288, DOY 295, and DOY 302 which represent the timing of the start of senescence, the middle of senescence, and the end of senescence, respectively.

decreased with chlorophyll concentration while leaf temperature remained constant (Fig. 3a, c). There was a clear photosynthetic rate decline between DOY 290 and DOY 294 during the measurements of the photosynthesis light response curve, indicating that leaf photosynthesis was inactivated since DOY 290 (Fig. 2).

Pigment concentrations declined during the entire observation period from DOY 259–304 (Fig. 3a). Both chlorophyll and carotenoids contents decreased from the maximum level (45.19 ± 12.77, 8.18 ± 1.72 μg/cm^2 on DOY 259) to $68.8 \pm 17.6\%$, $81.1 \pm 19.4\%$, respectively, on DOY 263. After this decline, these concentrations decreased at a lower rate. Both LAI and $Leaf_G$ were constant prior to DOY 263 and DOY 274, respectively, and then rapidly decreased after these dates (Fig. 3b, f).

Although chlorophyll and carotenoids concentration declined by 30% and 20%, respectively, from DOY 263 to 274, there was no sign of color change based on the G_{cc} change point analysis and visual inspection (Fig. 3). Meanwhile, the date of the first change point of the G_{cc} curve was consistent with the starting date of decreasing LAI, suggesting that the first change point of G_{cc} could indicate the starting decline of LAI in autumn well. We further examined the relationships between G_{cc} and the canopy foliar relative indices including LAI, $Leaf_O$, and $Leaf_F$ in the whole senescence period. $Leaf_O$ and $Leaf_F$ rates had a strong linear relationship with each other (Fig. 5d, $R^2 = 0.97$, $P < 0.001$), suggesting that the leaf number of marked branches has a good potential to serve as an effective indicator for the whole canopy. Our results also showed that G_{cc} had a highly linear relationship with $Leaf_F$ and $Leaf_O$ (Fig. 5a, $R^2 = 0.98$, $P < 0.001$; Fig. 5c, $R^2 = 0.98$, $P < 0.001$), measured via collected leaf litter in the boxes on the forest floor and the leaves counted on the marked branches. G_{cc} was also closely related to LAI in the period of senescence (Fig. 5b, $R^2 = 0.89$, $P < 0.001$).

To track variations in the relationships between G_{cc} and physiological traits across phenological stages requires the use of the

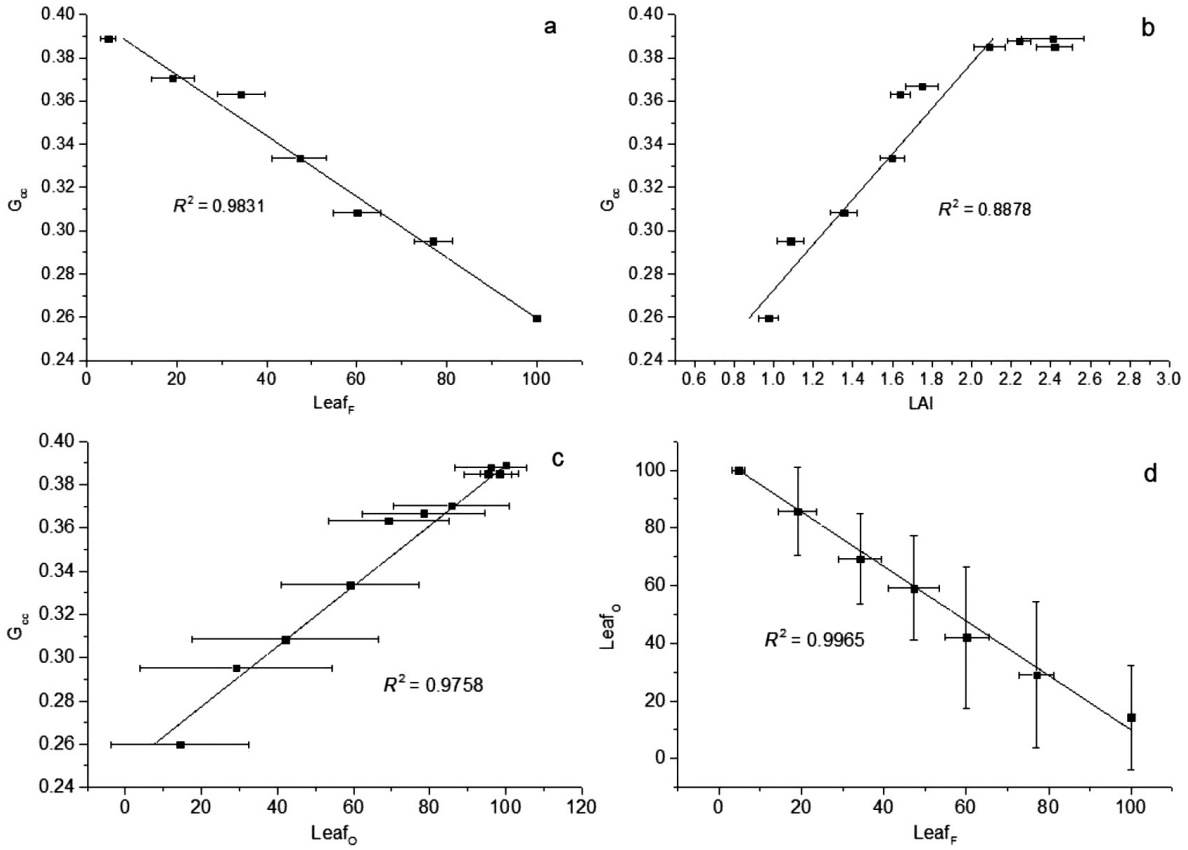

Fig. 5. Correlations between G_{cc} and Leaf$_F$ rate (a), collected by litter boxes, LAI (b), measured by LAI-2000, Leaf$_O$ rate (c), counted leaves number on labeled branches, and the relationship between Leaf$_F$ rate and Leaf$_O$ rate(d).

segmentation fitting methods to analyze these relationships due to the phenological transition in the senescence. The results demonstrated that G_{cc} had a close correlation with physiological traits (Chl, LAI*Chl, A_{max}, and LAI$_G$*A_{max}) when G_{cc} was equal or less than 0.36 (Fig. 6). Around the second G_{cc} change point in the autumn (DOY 289), G_{cc} declined to 0.36. The physiological traits in this period (Figs. 2, 3) and the declining G_{cc} around the second G_{cc} change point suggested the forest transitioned to lower photosynthetic activity before senescence. A_{max} remained at the 63.4 ± 20.1% of the maximum level (Fig. 3c); however, the LAI$_G$* A_{max} was only 23.8 ± 13.4% of its maximum level at the canopy level (Fig. 3c). For the period after DOY 290, photosynthetic rates remained at a low level (Fig. 2); chlorophyll concentration of leaves and canopy level were only 29.3 ± 17.0% and 13.5 ± 10.0% of their maximum level (Fig. 3a), respectively; Chl *a*:*b* was highly variable (109.2 ± 40.9%) and showed a declining trend (Fig. 3d).

After DOY 289, G_{cc} declined until DOY 295 which was the third change point from the BCP analysis (Fig. 3e). During this period, the chlorophyll content of leaves and at the canopy level accounted for only 18.6 ± 13.1% and 5.4 ± 5.1% of their maximum level (Fig. 3a), respectively. The rate of chlorophyll concentration declined after DOY 294, with carotenoids declining the fastest during this period (Fig. 3a). A_{max} and C_A_{max} also were at 20.1 ± 13.3% and 6.2 ± 5.6% of their maximum levels (Fig. 3c) on DOY 294, respectively, suggesting the end of growing season. Both A_{max} and LAI$_G$*A_{max} reached their lowest values (20.1 ± 13.3% and

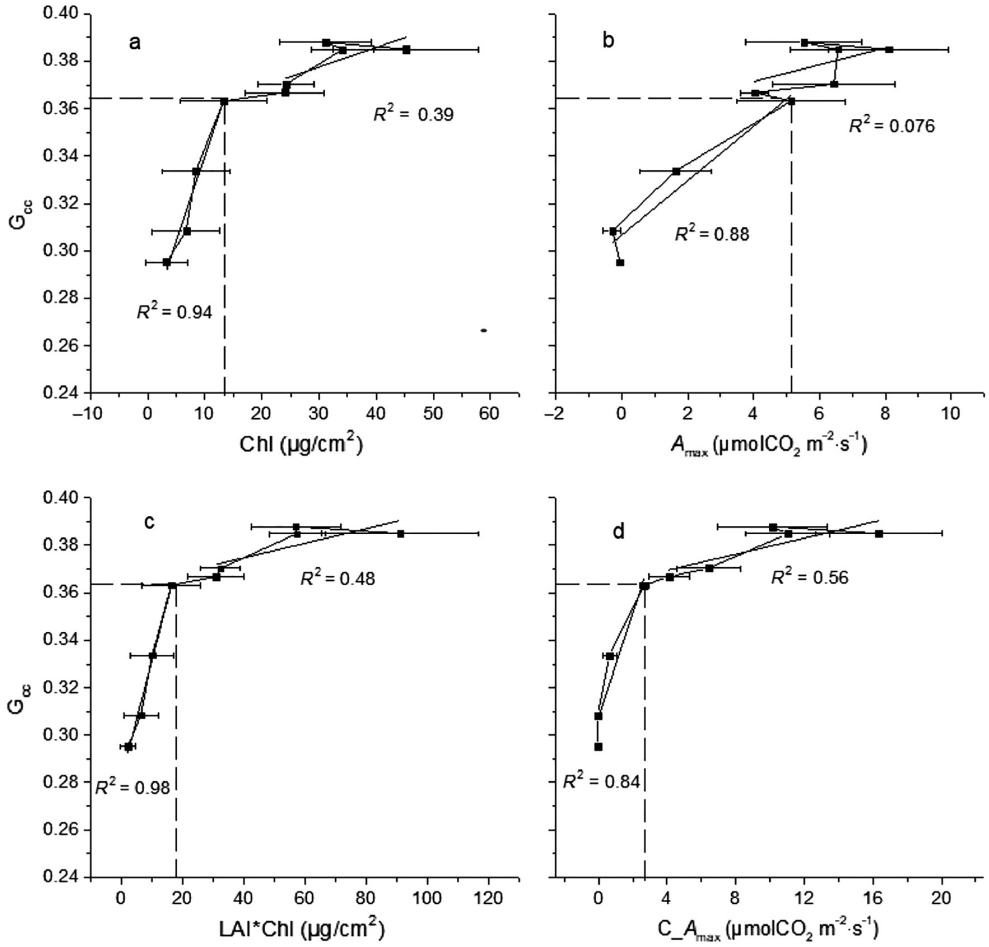

Fig. 6. Segmentally linear correlations between G_{cc} and foliar chlorophyll concentrations (a), and maximum photosynthesis rates on the leaf level (b), and canopy chlorophyll concentrations (c), and canopy maximum photosynthesis rates (d).

6.2 ± 5.6% of their maximum, respectively) in DOY 294 (Fig. 3c), but G_{cc} still accounted for 81.9% of its maximum in DOY 294 (Fig. 3e).

Discussion

Greenness indices derived from digital camera images, such as G_{cc}, have been widely applied to detect and quantify changes in canopy phenology (Richardson et al. 2009, Nagai et al. 2011, Sonnentag et al. 2012, Inoue et al. 2014, Toomey et al. 2015, Wingate et al. 2015, Brown et al. 2016,). In this study, we evaluated the potential of G_{cc} to detect phenological phase transitions and analyzed its correlations with physiological traits during the period of leaf senescence. Previous studies have shown that a substantial portion of uncertainty in detecting autumn phenological phases comes from mixed plant species and suggested that it is helpful to reduce uncertainty by monitoring species-specific characteristics with digital repeat photography in the foliage phenology (Inoue et al. 2014, Nagai et al. 2015, Wingate et al. 2015). The measurements in this study that focused on one single species significantly removed biases due to heterogeneous land covers. The single species reduced uncertainty in studying the autumn phenology phases extracted from digital repeat photography and physiological traits through the greenness index (G_{cc}). Our study suggests that G_{cc} could effectively detect the three critical points during the

senescence period, analyzed by the BCP approach, namely, (1) the start of senescence indicated by the decrease in LAI and the beginning of autumn leaf-off (DOY 268), (2) the initial stage of decreased photosynthetic activity (DOY 289), and (3) the end of growing season in deciduous broadleaf forests (DOY 295).

Our results demonstrated the ability of G_{cc} to detect the critical phenophases based on BCP approach, while fitting a logistic curve, as a common method in determining phenology, may lead to biases in the estimation of transition dates. For example, G_{cc} may have an unrealistic peak in the early spring which tends to cause a too early estimation of green-up with the fitting curve, and strong short-term fluctuations in the late autumn may also cause uncertainties in fitting the logistic curve (Henneken et al. 2013). We used the logistic curve proposed by Richardson et al. (2009) to fit G_{cc} as an example for discussing its limitation (Fig. 4). There is a big difference between the two methods. The physiological measurements showed that the canopy already progressed into the middle or even late stage of leaf senescence on DOY 288 (the start of senescence determined by the fitting logistic curve) and few yellow leaves remained with very low photosynthetic rates on DOY 295 (the middle of senescence determined by the fitting logistic curve). In contrast, in addition to these three critical phenology dates, the BCP approach captured one earlier dates (DOY 263) as the start of senescence that is not reflected by the logistic fitting.

Our study suggests the linkage between the canopy G_{cc} and leaf-scale senescence, based on leaf sampling. Our study site is a single species deciduous forest such that the sampled three trees could represent the entire forest situ. However, it is noted that G_{cc} only captures color changes from the top canopy in the broadband green channel. In general, the top of the canopy has more contribution to the G_{cc} in the dense forest with high LAI values, while the middle-to-low canopy also could have an impact on G_{cc} in the sparse forest with low LAI values. In this study, we focused on the phenological transition in the autumn, which included the phenological stages with both dense and sparse conditions. It is difficult to determine when and which layers of the canopy play a major role in regulating the G_{cc}, particularly when the senescence timing in the top and lower canopy may vary.

The ability of G_{cc} in tracking phenology generally depends on its sensitivity to canopy color, which is affected by both leaf chlorophyll concentration and LAI that acts as a scaling effect. However, the leaf color change may be invisible when saturated leaf chlorophyll concentration is slightly decreased. For example, at the early stage of senescence when leaf chlorophyll concentration decreased while LAI still remained stable, the G_{cc} time-series did not capture onset of chlorophyll degradation as the onset of senescence. With the further decrease of chlorophyll concentration, leaf color started to change and leaves also started to fall down (decreasing LAI), and then the G_{cc} decreased. It thus explained why the G_{cc} time-series can capture the onset of LAI decreasing but not the initial decrease of chlorophyll. Although our results suggest that G_{cc} is highly correlated with LAI as LAI stayed on the low level during the leaf-off period, it is still consistent with Keenan et al. (2014) that canopy greenness indices (e.g., G_{cc}) had a low sensitivity to changes in leaf area at high LAI levels: G_{cc} had no response to the decrease of LAI when LAI was >2.1 (Fig. 5b). The previous studies (Nagai et al. 2011, Keenan et al. 2014) showed that seasonal variation of G_{cc} has a close correlation with that of LAI during the leaf senescence, but the annual dynamic of G_{cc} has no significant correlation with that of LAI. Based on this evidence, G_{cc} is a reliable indicator to detect the date of LAI decline during canopy foliar senescence.

In addition, G_{cc} could also indicate leaf internal pigments change. Chlorophyll concentration is an important factor controlling the photosynthetic rate and thus gross primary productivity regardless of the environmental factors (Field and Mooney 1986, Morecroft et al. 2003). The decline of LAI was not necessarily correlated with the decline in photosynthetic rates at the leaf and canopy level (Fig. 3b, c; Keenan et al. 2014). The date when chlorophyll concentration begins to decrease in our study occurred earlier than the observed decline in LAI (Fig. 3). The G_{cc} curve did not detect the date of GPP began to decrease (Ahrends et al. 2009). Our results suggested that G_{cc} response could detect lower levels

of GPP as well as the end of the growing season. Previous studies showed a clear phenomenon relating the change of G_{cc} prior to minimal levels during the foliar senescence of deciduous canopies (Richardson et al. 2009, Sonnentag et al. 2012, Toomey et al. 2015, Brown et al. 2016). Our results suggested that 2nd change point may occur while plant canopy already exhibit low levels of photosynthesis rate (Fig. 3c) and chlorophyll concentration (Fig. 3a), which is in agreement with other studies (Ahrends et al. 2009, Mizunuma et al. 2013, Keenan et al. 2014). In addition, it had been shown that both the canopy level photosynthesis rate and foliar chlorophyll concentration (Fig. 3a, c) already finish the rapid decrease and stay in the minimum level in the date of 3rd change point of G_{cc}'s curve, which suggested that G_{cc} could detect the end of growing season by analyzing the downtrend rate during the senescence. Meanwhile, we are aware of several limitations in our results which should be addressed in further studies. For example, we only studied the single species deciduous forest such that it is not clear how mixed land cover types affect G_{cc}. We sampled three trees as the representation of the whole ROI and did not consider different contribution from the effects of physiological changes in the top and bottom layers on G_{cc}. More experiments are needed to quantify contribution from lower layers of the canopy to G_{cc} signals, and more studies about camera-based phenology and leaf physiological traits in various ecosystems should be also conducted in the future.

In the recent decade, digital camera imagery has been used for long-term, continuous ecological monitoring of plant canopies and to examine canopy response to environmental changes associated with climate change (Wingate et al. 2015, Brown et al. 2016, Moore et al. 2016). One of the most important and utilizable variables from this approach, G_{cc}, must be evaluated in tandem with field measurements of leaf-level physiological traits in order to assess plant function through the growing season. Our results show the G_{cc} can be used to estimate the canopy phenological transitional date, such as the leaf-off date and the ending date of growing season with a satisfactory accuracy. Our findings provide evidence for the application of camera-based phenology observation, with the help of quantitative analysis of the change points, to not only detect the phenological transition dates during leaf-off and senescence, but also to serve as a proxy represents changes in leaf physiological and functional traits during this period.

Acknowledgments

We thank Xi Yang for constructive suggestions of the experiments and Mary Heskel for constructive criticism of the manuscript. This research was funded by the Priority Academic Program Development of Jiangsu Higher Education Institutions in Discipline of Environmental Science and Engineer in Nanjing Forest University and China Scholarship Council No. 201506190095 to Z. Liu, and Brown University Seed Funds for International Research Projects on the Environment (to J. Tang). We also thank the Manuel F. Correllus State Forest of Massachusetts, the Nature Conservancy Hoft Farm Preserve, and Colbert for the permission to use the forests in the island of Martha's Vineyard in Massachusetts for our research.

Literature Cited

Ahrends, H. E., S. Etzold, W. L. Kutsch, R. Stoeckli, R. Bruegger, F. Jeanneret, H. Wanner, N. Buchmann, and W. Eugster. 2009. Tree phenology and carbon dioxide fluxes: use of digital photography at for process-based interpretation the ecosystem scale. Climate Research 39:261–274.

Asner, G. P., R. E. Martin, A. J. Ford, D. J. Metcalfe, and M. J. Liddell. 2009. Leaf chemical and spectral diversity in Australian tropical forests. Ecological Applications 19:236–253.

Brown, T. B., et al. 2016. Using phenocams to monitor our changing Earth: toward a global phenocam network. Frontiers in Ecology and the Environment 14:84–93.

Browning, D., J. Karl, D. Morin, A. Richardson, and C. Tweedie. 2017. Phenocams bridge the gap between field and satellite observations in an arid grassland ecosystem. Remote Sensing 9:1071.

Chen, X., and L. Xu. 2012. Phenological responses of *Ulmus pumila* (Siberian Elm) to climate change in the temperate zone of China. International Journal of Biometeorology 56:695–706.

Field, C. B., and H. A. Mooney. 1986. The photosynthesis-nitrogen relationship in wild plants. Cambridge University Press, New York, New York, USA.

Filippa, G., E. Cremonese, M. Galvagno, M. Migliavacca, U. M. di Cella, M. Petey, and C. Siniscalco. 2015. Five years of phenological monitoring in a Mountain grassland: inter-annual patterns and evaluation of the sampling protocol. International Journal of Biometeorology 59:1927–1937.

Foley, S., B. Rivard, G. A. Sanchez-Azofeifa, and J. Calvo. 2006. Foliar spectral properties following leaf clipping and implications for handling techniques. Remote Sensing of Environment 103:265–275.

Foster, D. R., B. Hall, S. Barry, S. Clayden, and T. Parshall. 2002. Cultural, environmental and historical controls of vegetation patterns and the modern conservation setting on the island of Martha's Vineyard, USA. Journal of Biogeography 29:1381–1400.

Fu, Y. H., H. Zhao, S. Piao, M. Peaucelle, S. Peng, G. Zhou, P. Ciais, M. Huang, A. Menzel, and J. Peñuelas. 2015. Declining global warming effects on the phenology of spring leaf unfolding. Nature 526:104–107.

Gitelson, A. A., Y. Gritz, and M. N. Merzlyak. 2003. Relationships between leaf chlorophyll content and spectral reflectance and algorithms for non-destructive chlorophyll assessment in higher plant leaves. Journal of Plant Physiology 160:271–282.

Henneken, R., V. Dose, C. Schleip, and A. Menzel. 2013. Detecting plant seasonality from webcams using Bayesian multiple change point analysis. Agricultural and Forest Meteorology 168:177–185.

Ide, R., and H. Oguma. 2010. Use of digital cameras for phenological observations. Ecological Informatics 5:339–347.

Ide, R., and H. Oguma. 2013. A cost-effective monitoring method using digital time-lapse cameras for detecting temporal and spatial variations of snowmelt and vegetation phenology in alpine ecosystems. Ecological Informatics 16:25–34.

Inoue, T., S. Nagai, T. M. Saitoh, H. Muraoka, M. N. Nasahara, and H. Koizumi. 2014. Detection of the different characteristics of year-to-year variation in foliage phenology among deciduous broad-leaved tree species by using daily continuous canopy surface images. Ecological Informatics 22:58–68.

Kampe, T. U., B. R. Johnson, M. Kuester, and M. Keller. 2010. NEON: the first continental-scale ecological observatory with airborne remote sensing of vegetation canopy biochemistry and structure. Journal of Applied Remote Sensing 4:043510.

Keenan, T. F., et al. 2014. Tracking forest phenology and seasonal physiology using digital repeat photography: a critical assessment. Ecological Applications 24:1478–1489.

Lichtenthaler, H. K., and C. Buschmann. 2001. Chlorophylls and carotenoids: measurement and characterization by UV-VIS Spectroscopy. Current protocols in food analytical chemistry. John Wiley & Sons, New York, New York, USA.

Lieth, H. 1974. Phenology and seasonality modeling. Springer-Verlag, New York, New York, USA.

Liu, Q., Y. H. Fu, Z. Zhu, Y. Liu, Z. Liu, M. Huang, I. A. Janssens, and S. Piao. 2016. Delayed autumn phenology in the Northern Hemisphere is related to change in both climate and spring phenology. Global Change Biology 22:3702–3711.

Liu, Z., H. Hu, H. Yu, X. Yang, H. Yang, C. Ruan, Y. Wang, and J. Tang. 2015. Relationship between leaf physiologic traits and canopy color indices during the leaf expansion period in an oak forest. Ecosphere 6:art259.

Matiu, M., L. Bothmann, R. Steinbrecher, and A. Menzel. 2017. Monitoring succession after a non-cleared windthrow in a Norway spruce mountain forest using webcam, satellite vegetation indices and turbulent CO2 exchange. Agricultural and Forest Meteorology 244:72–81.

Menzel, A. 2002. Phenology: its importance to the global change community. An editorial comment. Climatic Change 54:379–385.

Mizunuma, T., M. Mencuccini, L. Wingate, J. Ogee, C. Nichol, and J. Grace. 2014. Sensitivity of colour indices for discriminating leaf colours from digital photographs. Methods in Ecology and Evolution 5:1078–1085.

Mizunuma, T., M. Wilkinson, E. L. Eaton, M. Mencuccini, J. I. L. Morison, and J. Grace. 2013. The relationship between carbon dioxide uptake and canopy colour from two camera systems in a deciduous forest in southern England. Functional Ecology 27:196–207.

Moore, C. E., et al. 2016. Australian vegetation phenology: new insights from satellite remote sensing and digital repeat photography. Biogeosciences Discuss 2016:1–30.

Morecroft, M. D., V. J. Stokes, and J. I. L. Morison. 2003. Seasonal changes in the photosynthetic capacity of canopy oak (*Quercus robur*) leaves: the impact of slow development on annual carbon uptake. International Journal of Biometeorology 47:221–226.

Nagai, S., T. Ichie, A. Yoneyama, H. Kobayashi, T. Inoue, R. Ishii, R. Suzuki, and T. Itioka. 2016. Usability of time-lapse digital camera images to detect characteristics of tree phenology in a tropical rainforest. Ecological Informatics 32:91–106.

Nagai, S., T. Inoue, T. Ohtsuka, S. Yoshitake, K. N. Nasahara, and T. M. Saitoh. 2015. Uncertainties involved in leaf fall phenology detected by digital camera. Ecological Informatics 30:124–132.

Nagai, S., T. Maeda, M. Gamo, H. Muraoka, R. Suzuki, and K. N. Nasahara. 2011. Using digital camera

images to detect canopy condition of deciduous broad-leaved trees. Plant Ecology & Diversity 4:79–89.

Nasahara, K. N., and S. Nagai. 2015. Review: Development of an in situ observation network for terrestrial ecological remote sensing: the Phenological Eyes Network (PEN). Ecological Research 30:211–223.

Penuelas, J., T. Rutishauser, and I. Filella. 2009. Phenology feedbacks on climate change. Science 324:887–888.

Piao, S., et al. 2008. Net carbon dioxide losses of northern ecosystems in response to autumn warming. Nature 451:49–52.

Pope, K. S., V. Dose, D. Da Silva, P. H. Brown, C. A. Leslie, and T. M. Dejong. 2013. Detecting nonlinear response of spring phenology to climate change by Bayesian analysis. Global Change Biology 19:1518–1525.

Richardson, A. D. R.. 2012. Terrestrial biosphere models need better representation of vegetation phenology: results from the North American Carbon Program Site Synthesis. Global Change Biology 18:566–584.

Richardson, A. D., B. H. Braswell, D. Y. Hollinger, J. P. Jenkins, and S. V. Ollinger. 2009. Near-surface remote sensing of spatial and temporal variation in canopy phenology. Ecological Applications 19: 1417–1428.

Richardson, A. D., J. P. Jenkins, B. H. Braswell, D. Y. Hollinger, S. V. Ollinger, and M.-L. Smith. 2007. Use of digital webcam images to track spring green-up in a deciduous broadleaf forest. Oecologia 152:323–334.

Richardson, A. D., et al. 2018. Tracking vegetation phenology across diverse North American biomes using PhenoCam imagery. Scientific Data 5:180028.

Ryu, Y., J. Verfaillie, C. Macfarlane, H. Kobayashi, O. Sonnentag, R. Vargas, S. Ma, and D. D. Baldocchi. 2012. Continuous observation of tree leaf area index at ecosystem scale using upward-pointing digital cameras. Remote Sensing of Environment 126:116–125.

Sakamoto, T., A. A. Gitelson, A. L. Nguy-Robertson, T. J. Arkebauer, B. D. Wardlow, A. E. Suyker, S. B. Verma, and M. Shibayama. 2012. An alternative method using digital cameras for continuous monitoring of crop status. Agricultural and Forest Meteorology 154–155:113–126.

Sonnentag, O., K. Hufkens, C. Teshera-Sterne, A. M. Young, M. Friedl, B. H. Braswell, T. Milliman, J. O'Keefe, and A. D. Richardson. 2012. Digital repeat photography for phenological research in forest ecosystems. Agricultural and Forest Meteorology 152:159–177.

Tang, J., C. Körner, H. Muraoka, S. Piao, M. Shen, S. J. Thackeray, and X. Yang. 2016. Emerging opportunities and challenges in phenology: a review. Ecosphere 7:e01436.

Thomson, J. R., W. J. Kimmerer, L. R. Brown, K. B. Newman, R. M. Nally, W. A. Bennett, F. Feyrer, and E. Fleishman. 2010. Bayesian change point analysis of abundance trends for pelagic fishes in the upper San Francisco Estuary. Ecological Applications 20:1431–1448.

Toomey, M., et al. 2015. Greenness indices from digital cameras predict the timing and seasonal dynamics of canopy-scale photosynthesis. Ecological Applications 25:99–115.

Vitasse, Y., S. Delzon, E. Dufrêne, J.-Y. Pontailler, J.-M. Louvet, A. Kremer, and R. Michalet. 2009. Leaf phenology sensitivity to temperature in European trees: Do within-species populations exhibit similar responses? Agricultural and Forest Meteorology 149:735–744.

Westergaard-Nielsen, A., M. Lund, S. H. Pedersen, N. M. Schmidt, S. Klosterman, J. Abermann, and B. U. Hansen. 2017. Transitions in high-Arctic vegetation growth patterns and ecosystem productivity tracked with automated cameras from 2000 to 2013. Ambio 46:S39–S52.

Wingate, L., et al. 2015. Interpreting canopy development and physiology using a European phenology camera network at flux sites. Biogeosciences 12:5995–6015.

Woebbecke, M. D., E. G. Meyer, K. Von Bargen, and A. D. Mortensen. 1995. Color indices for weed identification under various soil, residue, and lighting conditions. Transactions of the ASAE 38:259.

Yang, X. 2014. The times they are a-changin': scaling seasonality of plant physiology from leaf to satellite and implications for terrestrial carbon cycle. Brown University, Providence, Rhode Island, USA.

Yang, X., J. F. Mustard, J. Tang, and H. Xu. 2012. Regional-scale phenology modeling based on meteorological records and remote sensing observations. Journal of Geophysical Research-Biogeosciences 117:G03029.

Yang, X., J. Tang, and J. F. Mustard. 2014. Beyond leaf color: comparing camera-based phenological metrics with leaf biochemical, biophysical, and spectral properties throughout the growing season of a temperate deciduous forest. Journal of Geophysical Research-Biogeosciences 119:181–191.

Yang, X., J. Tang, J. F. Mustard, J. Wu, K. Zhao, S. Serbin, and J.-E. Lee. 2016. Seasonal variability of multiple leaf traits captured by leaf spectroscopy at two temperate deciduous forests. Remote Sensing of Environment 179:1–12.

Yang, H., X. Yang, M. Heskel, S. Sun, and J. Tang. 2017. Seasonal variations of leaf and canopy properties tracked by ground-based NDVI imagery in a temperate forest. Scientific Reports 7:1267.